The influence of SAMA seasonality on diurnal variation of the magnetic field in oceanic islands of the Southern Hemisphere

Hermes, F.C.M., ON/UFF; Benyosef, L.C.C, ON; Souza, G.S.; UFF

Abstract

In this work it used data from six magnetic observatories (TDC, PIL, KEP, ASC, IPM and VSS). All of them are located in the magnetic southern hemisphere below the DIP Equator and one (PIL) is located near the center of the SAMA. The observatory (VSS) is on the SAMA's northeast border ASC, TDC and KEP are islands located in the South Atlantic Ocean and IPM in the South Pacific Ocean. These results are the first from a study of the influence of the geology at the locations and the SAMA on diurnal variation in oceanic islands and in mainland stations at low and medium latitudes.

Introduction

Chapman in 1951 suggested the existence of a narrow band of electric current flowing in the diurnal part of the day, eastward, at an average altitude of 100 km and at +-3° with respect to the equatorial dip. This region is called the Equatorial Electrojet (EEJ) and is global in scope. In the same region arise electrical currents flowing in the opposite direction, a phenomenon called Counter-Electrojet (CEJ).

This paper analyzes the influence of the Magnetic Anomaly of the South Atlantic (AMAS = SAMA) on the diurnal variation of the horizontal components (H) and (Z) of the geomagnetic field south of the equatorial dip in the period of the year 2015. The results obtained are associated with the presence of the EEJ and solar activity considering that changes in the amplitude and phase of the diurnal variation occur due to solar activity. In this study we are also including the increasing influence of this anomaly in regions of the Pacific Ocean considering its relative fast displacement of 0.3° per year. Thus, we analyze the regions formed by islands around the South American continent including the southern parts of the Atlantic and South Pacific Oceans as being of special scientific interest especially as they are under the influence of the most extensive magnetic anomaly of the Earth's magnetic field (CMT), the AMAS, which has its lowest intensities compared to any other region in the world. Thus, much research is done to study its displacement, area of coverage, variation in intensity, and its influence on other nearby regions. One way to evaluate changes in the positioning and intensity of the field is achieved by analyzing these variations recorded at different locations in its range. We use data from the magnetic observatories at Tristan da Cunha (TDC), Pilar (PIL), King Edward Point (KEP), Vassouras (VSS), Ascension Island (ASC) and Mataveri Easter Island (IPM). The records from the observatories were worked out in IAGA format (1 minute). All information about the observatories can be found in Table 1.

Table 1 - Location of the magnetic stations

Code	Geographic Latitude	Geographic Longitude
TDC	37° 06' 00" S	12° 17' 00" W
PIL	31° 40' 44"S	63° 52' 46" W
KEP	54° 17' 01" S	36° 29' 45" W
ASC	7° 56' 30" S	14° 21' 45" W
VSS	22° 24' 16" S	43° 39' 48" W
IPM	27° 17' 13" S	109° 42' 00" W

Figure 1 shows the geographical distribution of the stations in this work.

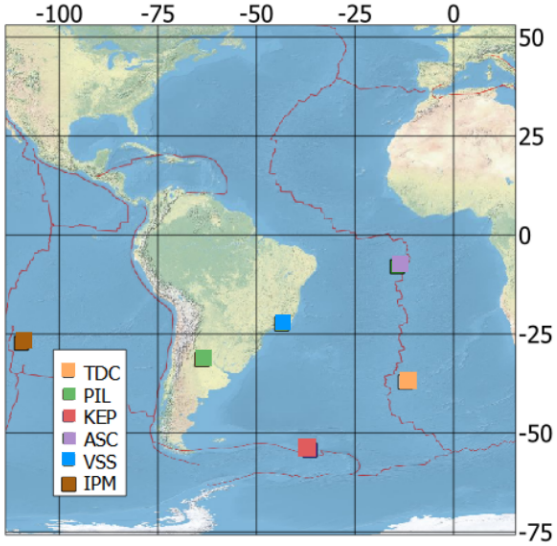

Figure 1. Geographical location of the magnetic stations under study.

Geology

The volcanic nature of these islands can influence the magnetic records of the Z component, even if it is a very

small influence, because of the magnetic susceptibility of the magmatic rocks on the island. We intend to correlate these results with the geology of the four observatories selected, which was succinctly described. The geology of the islands TDC, ASC, KEP, islands located in the Atlantic Ocean and IPM, located in the Pacific Ocean, is considered. The British Overseas Territory of Ascension Island and Tristan da Cunha (and Saint Helena) is made up of some of the remotest islands on earth. It spans a huge distance of 3,642km and runs along the Mid Atlantic Ridge in the South Atlantic Ocean. All the islands are volcanic, but are formed by hotspots rather than being part of the ridge itself. The hotspot that created Tristan da Cunha was probably involved in the spitting up of the supercontinent of Gondwanaland, some 135mya. Flood basalts exist in modern day Parana, Brazil, Etendeka and Namibia, and erupted when the two places were connected, but began to split apart. As the south Atlantic has spread apart, a series of ancient Tristan da Cunha's were formed, their eroded stumps are now the shallower areas of the Walvis Ridge and Rio Grande Rise. However, Ascension Island is different and has no chain of seamounts or islands. In fact, Ascension lies on the South American plate, while the hotspot is on the other side of the Mid Atlantic Ridge under the African plate, and the magma flows along the ridge to reach Ascension Island. The chemistry of the lava on each island is different, showing each hotspot derives from a different source. The Tristan lavas contain the chemical signature of sediments, which perhaps adds weight to the subducted plate idea. The Ascension lavas show they have been heavily mixed by lavas from the Mid Atlantic Ridge (Weaver's website).

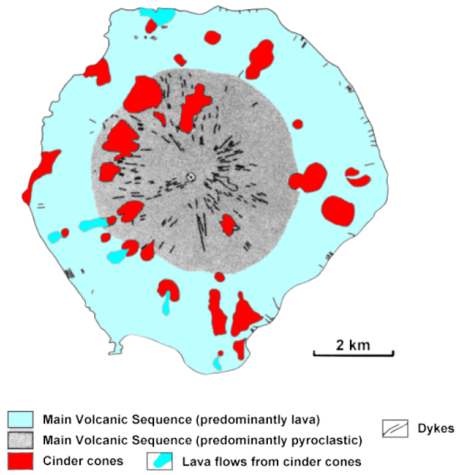

Fig 2. A simplified geological map of Tristan da Cunha. Taken from Barry Weaver's website, originally adapted from Baker et al. (1964).

From whatever direction the island is approached its coasts are rock bound, and more or less precipitous. No open beach or detrital flat exists anywhere on its outer margin. There is a valley about a mile wide in Moraine Flat, which runs up from the enclosed south-west rim of Cumberland Bay, near King Edward's Cove, for about 4 miles to an ice-field and glacier. There are also several patches of detrital flats and moraines, which probably occupy hollows scooped out by glacial action. Leith Harbour is one of these ; Husvik Harbour, where the Bucentaur Whaling Company is located, is another ; Elsie Harbour and Adventure Harbour, on the northwest corner of the island, originally scooped out by ice into one channel, have been separated into two safe refuge anchorages by morainic detritus blocking up several miles of its center.

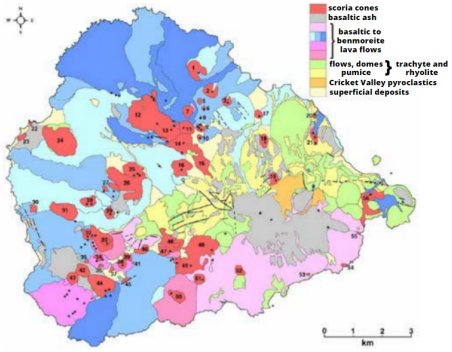

Figure 3. Geological map of Ascension Island

The coast, always rock bound, has generally a stern and rugged appearance, not unlike parts of the north-west Highlands of Scotland. Along the north-east coast, running from north-west to south-east, the outer escarpments are succeeded inland by rocky heights, having ice-fields in every hollow, and eventually culminate in the central or Allardyce range of mountains. The central range, except in steep rock escarpments and splintery crests, is covered with a permanent cap of ice-fields and snow. Mount Paget, the highest point of the central range, 8383 feet above sea-level, has almost vertical escarpments of gnarled rusty-brown rocks which reach to its summit; the escarpments are surrounded by ice-fields and glaciers, which slowly flow down to the edge of the Nordenskjold, Moraine Fiord, and Moraine Flat Glaciers in Cumberland Bay.

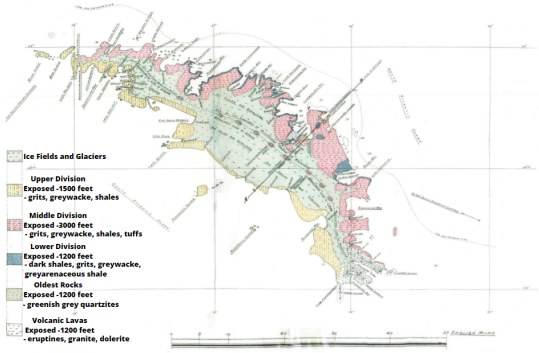

Figure 4. Geological map of South Georgia(KEP)

Easter Island (Rapa Nui, Chile) is an intraoceanic volcanic island on the Easter hotspot, ~350 km E of the Eastern Pacific Rise. We match new field data with previously published age and petrochemical data to

reconstruct the general evolution of the Island. This consists of three main volcanoes (Poike, Rano Kau, and the larger Terevaka), which experienced an overall similar and nearly coeval evolution, characterized by two periods: (1) buildup of a basaltic shield, culminating in the development of a summit caldera and the emission of more evolved highly porphyritic lavas (ca. 0.78–0.3 Ma); and (2) rifting along the shield flanks, by means of fissure eruptions (0.24–0.11 Ma). The trend of most eruptive fissures, NNE-SSW to NE–SW, appears to be controlled by the ~NE-SW elongated, emerged, and submerged morphology of the island. However, while the fissure-forming period at Rano Kau and Poike appears to be associated with reduced magma supply to the reservoir, at Terevaka it is characterized by the arrival of new basic magma, rejuvenating the system. The comparison to other intraoceanic volcanic islands suggests that, because of its tectonomagmatic features (low eruptive rate, scattered rift zones, and scarce lateral collapses), Easter Island represents an end-member type of hotspot volcano.

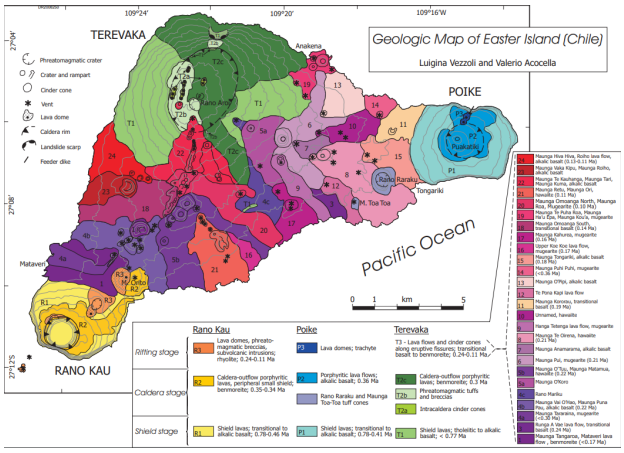

Figure 5. Geological map of Easter Island (Chile)

Methodology

In this analysis, we are considering six stations: TDC, PIL, KEP, ASC, VSS and IPM over the period of one year (2015). In addition, we are using only extremely quiet days, and to make the final selection, we use the Kp index, which is a global index, and choose a day with very little geomagnetic activity. The Kp index is the global index of geomagnetic storms and is based on three-hour measurements of the K-indices, for a given value (Du, D. et al., 2010). The Kp index measures the deviation of the horizontal most disturbed magnetic field component at fixed stations around the world with its own local K-index. The result is the global Kp index. The Kp index ranges from 0 to 9 on a quasi-logarithmic scale, where a value of 0 means that there is very little geomagnetic activity and a value of 9 shows an extreme geomagnetic storm (Wanliss, J. A. et al., 2014).

Magnetometers were used to generate the records made with fluxgate type vectors, with a period of second and converted to minute. This instrument records the three components of the geomagnetic field (X, Y, and Z). The data were processed using Python. The diurnal variation of the geomagnetic field at low latitudes is associated with the steady flow of the solar wind. The variability occurs at all hours of the day. Its magnitudes in the D, H, and the Z components have the same diurnal variation, which peaks at noon as the Sq(H) at low latitudes, and a weak seasonal variation that peaks at the June solstice (local summer). Results from previous studies suggest that ionospheric conductivity primarily controls the electric field and solar winds control the phase and randomness of the day-to-day variability of hourly Sq amplitudes (Okeke F.N., et al., 1998).

Sq can undergo variation because of the South Atlantic Magnetic Anomaly (SAMA), which is one of the most important anomalies in the geomagnetic field. It is caused by the non-centrality of the Earth and its magnetic dipole. Continuously changing in space and time, SAMA covers most of the South Atlantic Ocean and parts of South America, South Africa and Antarctica (Badhwar G., 1997). The center of SAMA is taken as the locus of minimum intensity in the South Atlantic, with a minimum value around 22,500 nT and is now located near the city of Asuncion, Paraguay. The effect of SAMA can be observed by some Latin American geomagnetic observatories. The Vassouras Magnetic Observatory (VSS) in Brazil and Pilar (PIL) in Argentina provide measurements where it is possible to observe that the influence of SAMA is apparent.(Hartmann, G. A., & Pacca, I. G. 2009).

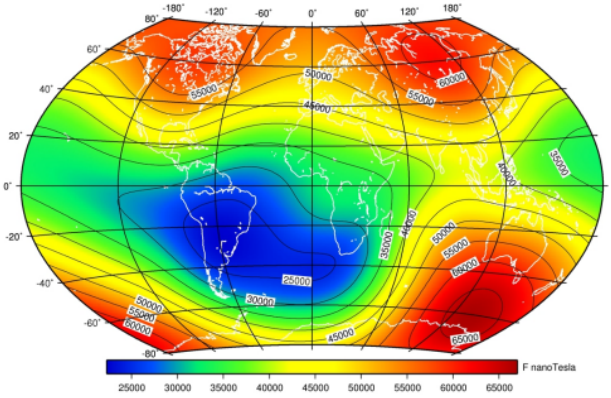

Figure 6. Total magnetic field strength in 2015.

In the quiet period of the day the baseline dH, according to Yamazaki, Y et al, is evaluated considering only the period when the E layer of the ionosphere practically disappears, that is, only the average of the horizontal component in the six nighttime hours is considered: 00.00, 01.00, 02.00, 22.00, 23.00 and 24.00.

$$dH = H(LT) - \frac{H(0)+H(1)+H(2)+H(22)+H(23)+H(24)}{6} \quad (1)$$

Thus, the diurnal variation, for each day, is considered based on equation (1) and this model assumes that during the night, in magnetically calm conditions, the currents in the ionosphere are very small and the conductivity in the E region practically disappears during the night except at auroral latitudes. The diurnal variation

obtained for the four chosen calm days of the year 2015 for the H and Z components is shown in Figures 9 and 10.

Results and Discussion

For the analysis of the horizontal component (H) in the year 2015, the Schwabe Solar Cycle, popularly known only as the solar cycle, which is the cycle with a series of determined phenomena of the Sun that occur at intervals of approximately eleven years, was considered.

The current cycle is number 25, and 2015 falls within solar cycle 24, which was from January 4, 2008 and lasted until December 2019. The storm on March 17, 2015 was the most intense storm that occurred during cycle 24 (Dst = -222nT). Figure 7 presents the progression of the solar cycle.

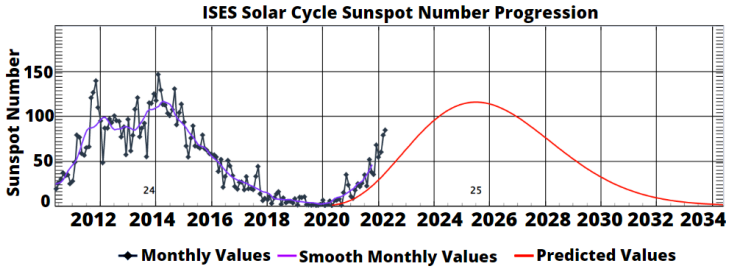

Figure 7. Progression of the solar cycle.

It is in agreement with Nair and Nayar (2009) conclusions, that geomagnetic activity is associated with coronal holes and enhances at declining phase of solar cycle. This conclusion also agrees with Zhao and Zong (2012), who show that geomagnetic activity is higher around equinoxes and maximal during positive polarity epochs.

Despite that proton flux variability has been studied in the past [Zou et al. 2015], electron precipitation effects into the SAMA are not well understood yet. Moreover, there is some evidence of their influence into the geomagnetic variability [Jayanthi et al. 1997a] .

As the main field continues decreasing inside the SAMA, more particles from the inner radiation belt will precipitate as a result of the broadening of the trapped particles loss cone. This will enhance the risk of radiation exposure on crews and equipments in flight through this area. In this way, the SAMA shares some unique features with the auroral zones where the particle precipitation plays an important role regarding the energy influx into the ionosphere.

Figure 8 shows the period of the year 2015 where the diurnal variation for the magnetic stations of TDC, KEP, ASC, VSS, PIL that starts the data without errors on 02/17 and the IPM station had its data recorded until 09/15 without errors. In Figure 8 the points in gray represent the selected quiet days: 03/18/2015, 06/23/2015, 08/27/2015 and 12/21/2015.

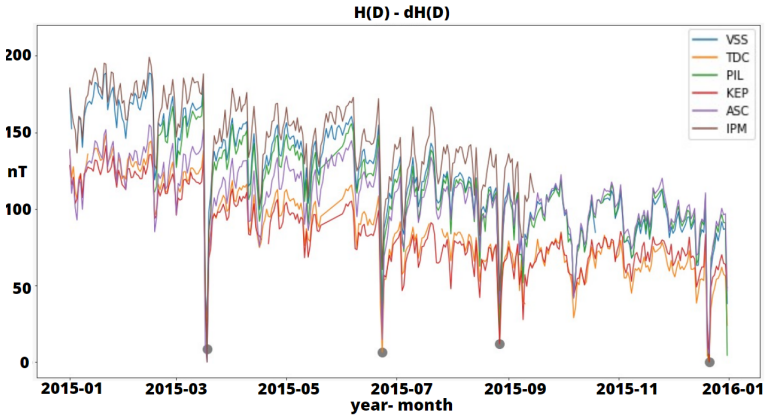

Figure 8. H(D)-dH(D) in the year 2015 for the selected stations

In the graph it is shown that the diurnal variation for the IPM, VSS, PIL and ASC stations present the same morphology, with higher values than the diurnal variation of the TDC and KEP stations, which present a morphology with lower values for the whole year.

Due to the Earth's inclination angle of 23º 27' and the translation movement, which occurs around the Sun, we have the change of seasons. This happens because, during the translation movement, which lasts one year, the incidence of sunlight is different in each region, due to the inclination of the planet. Table 2 shows the dates of the seasons during the study period.

Table 2 - 2015 seasons

Season	Started in the year 2015
Fall	03/20
Winter	06/21
Spring	09/23
Summer	12/22

The selected quiet days are in late fall (3/18), early winter (6/23), mid-winter (8/27), and the last day of spring (12/21). Figure 10 presents the diurnal variation of dH(D)-H(LT) of the quiet days of the year 2015.

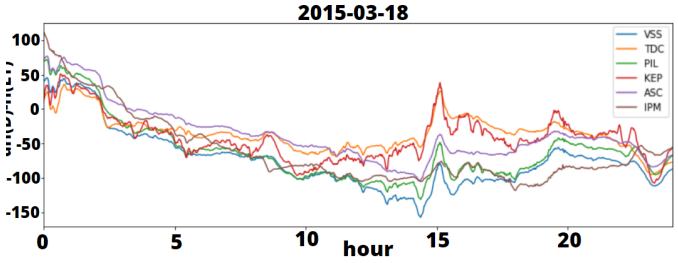

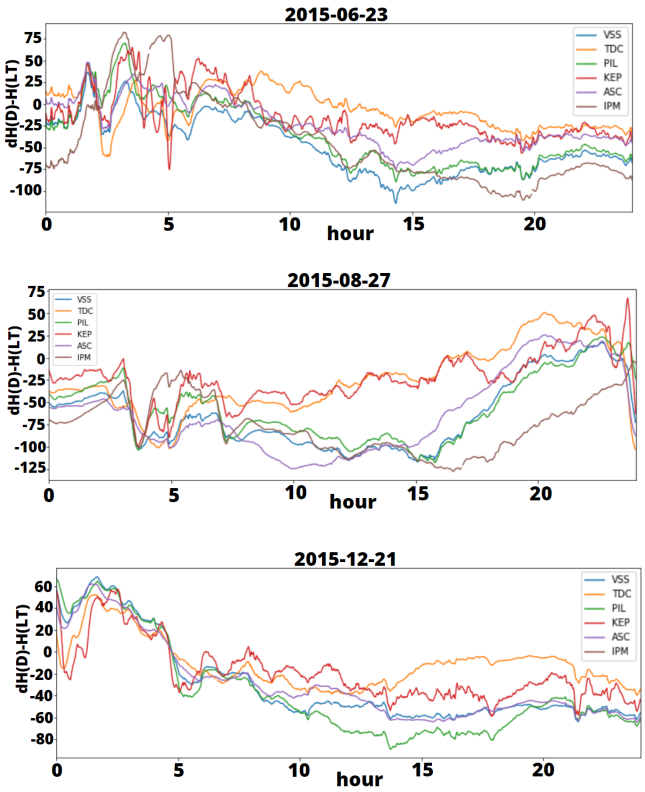

Figure 9. The diurnal variation of dH(D)-H(LT) of the quiet days in the year 2015.

The plot in Figure 9 with the magnetically quiet day 03/18 shows that the diurnal variation for the TDC and KEP stations presents the same morphology, with their peaks in the 3 o'clock hour higher than that of the ASC, PIL, VSS and IPM stations which presents the peak morphology different from the others. The PIL and VSS stations are the closest to the center of SAMA and ASC is the station closest to the equatorial dip (EEJ).

It can be observed that in the graphs of the calm days 06/23/2015, 08/27/2015 and 12/21/2015 the morphology of TDC and KEP as well as in the first calm day discussed presents with higher values than ASC, PIL, IPM and VSS. On 06/23/06 the peak of the morphology of the stations occurs in the early morning, IPM presents an anomalous peak of the other stations around 5 o'clock and together with VSS has the morphologies with lower values that occur at different times.

It presents on day 08/27 ASC, VSS, IPM and KEP morphologies with lower values, and on day 12/21 the peak occurred in the morning, with solar activity decaying after 5 am for all stations, except IPM that the data of this day were in error. Figure 10 presents the diurnal variation of dZ(D)-Z(LT) of the quiet days of the year 2015.

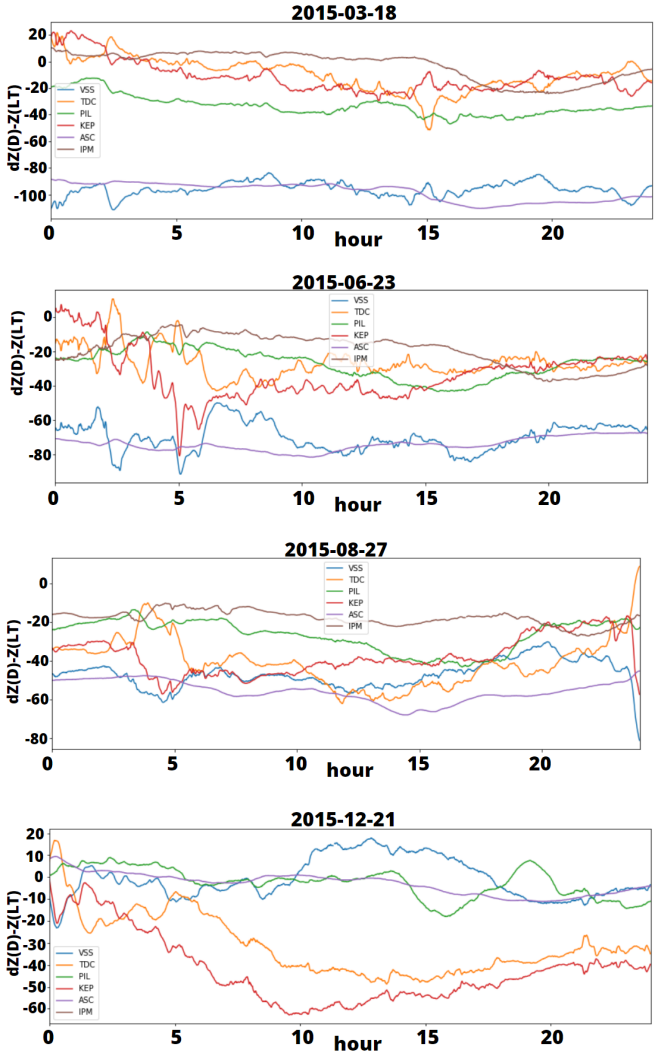

Figure 10. The diurnal variation of dZ(D)-Z(LT) of the quiet days of the year 2015..

The graph of Figure 10 with the magnetically quiet day 03/18 shows that the diurnal variation of the Z component for the pair of stations TDC and KEP has a similar morphology and with peaks with opposite directions in the hours of 15 hours and around 23 hours; the pair PIL and IPM presents similar average values higher than the pair of stations ASC and VSS that presents the morphology with lower values of the others. It can be observed that in the graphs of the calm days 06/23/2015, 08/27/2015 the morphology of TDC, PIL, IPM and KEP as well as in the first calm day approached presents with higher values than ASC and VSS. On 6/23 KEP presents a peak before 4 o'clock that suffers a decay in its morphology with opposite direction to the peak of the TDC station. On 12/21 VSS, ASC and PIL had higher morphologies than TDC and KEP, and the IPM data for this day were in error and were excluded from the analysis. The amplitude of the diurnal variation for the H and Z components were plotted on the graphs in Figure 11.

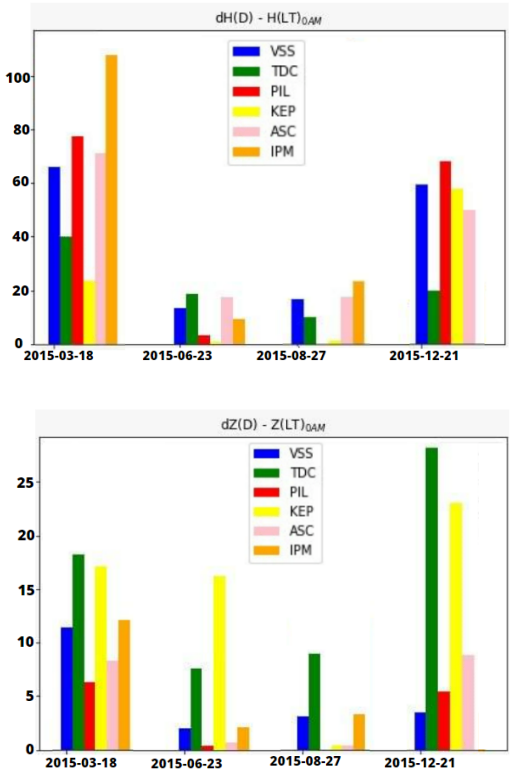

Figure 11. Amplitude in nT of the diurnal variation of H(D)-dH(D) and of dZ(D)-Z(LT) of the quiet days of the year 2015

From the analysis of the graphs in Figure 11, it can be seen that the amplitude of diurnal variation is not constant but varies according to the location, and there is a large variability between the selected days of H amplitude where on 03/18 among the stations, IPM appears with the highest amplitude, and on days 06/23 and 08/27 the values of the amplitudes are lower, up to a maximum of 30 nT. In the graph of the amplitudes of the Z component of the magnetic stations, TDC and KEP present themselves with the highest values. The PIL station does not present values on day 08/27 and the IPM station does not have data for day 12/21. The graphs of H and Z amplitudes are important for understanding the interference of SAMA on magnetic stations on the South American continent that are in the center of it (PIL) and on its edge (VSS), and of stations near the equatorial electrojet (ASC).

Conclusions

The present work showed that the morphology of the curves obtained for Z might be interpreted to be due to the Equatorial Electrojet (EEJ) and the SAMA. It can be seen that the variation in the Z component is a result of the great influence of the Sq current system and in a smaller scale it is due to induction effects in the ocean (Kuvshinov et al., 2007). The geological influence is a little perceptible in the graphs seen, because it is very small when compared with the Sq system. The EEJ can enhance the Sq current system in the equatorial region, however, a kind of phase difference was observed between the six stations studied. This phase shift may be attributed to the differences in their latitudinal locations. The data of the Z component from ASC, KEP, TDC and IPM can be a problem in some cases, because of all the variations in the magnetization that a volcanic island can have. The pattern obtained in the curves revealed that H has deviated from the normal known variation of morning trough and afternoon crest. This could be attributed to change in the magnetosphere electric field (Okeke et al., 1998). The results of this preliminary study confirm that the morphology of the curves obtained for H and Z on ASC can be related to the SAMA, as well as the curves of ASC and TDC can be attributed to the EEJ. For a better understanding of the geological influence in the curves, it will be necessary for future work a statistical analysis using the frequency domain in the same diurnal variation for comparison with the depth of the crust, and a model will be made aggregating all of these influences.

Acknowledgements

The authors thank the Observatório Nacional (Rio de Janeiro, Brazil) and MCTIC for financial support. In addition, we thank INTERMAGNET for providing the data from the stations used in the work.

References

Chapman S 1951 The equatorial electrojet as detected from the abnormal electric current distribution above Huancayo, Peru and elsewhere; Arch.Meterol.Geophys.BioklimatolA4 368–390.

Finlay, C.C., N. Olsen and L. Tøffner-Clausen (2015) DTU candidate field models for IGRF-12 and the CHAOS-5 geomagnetic field model. Earth Planets and Space, 67:114

Freire, L., Laranja, S. R. and Benyosef, L, 2016. Geomagnetic Field Variations in the Equatorial Electrojet Sector, VII Simpósio Brasileiro de Geofísica.

International Service of Geomagnetic Indices. Disponível no URL: http://isgi.latmos.ipsl.fr/lesdonne.htm

Hartmann, Gelvam A.; Pacca, Igor G. (2009). Time evolution of the South Atlantic Magnetic Anomaly. Anais da Academia Brasileira de Ciências, 81(2), 243–255

Kuvshinov, A., C. Manoj, N. Olsen, and T. Sabaka (2007), On induction effects of geomagnetic daily variations from equatorial electrojet and solar quiet sources at low and middle latitudes, J. Geophys. Res., 112, B10102

Luigina Vezzoli, Valerio Acocella; Easter Island, SE Pacific: An end-member type of hotspot volcanism. *GSA Bulletin* 2009;; 121 (5-6): 869–886

Weaver, B. 2002: A Guide to the geology of Ascension Island and Saint Helena, ebook

Yamazaki, Y., et al., 2011. An empirical model of the quiet daily geomagnetic field variation, Journal of Geophysical Research, 116, A10311